

## Scaling behavior for the pressure and energy of shearing fluids

Jialin Ge, B. D. Todd,\* Guangwen Wu, and Richard J. Sadus

Centre for Molecular Simulation, Swinburne University of Technology, P.O. Box 218, Hawthorn, Victoria 3122, Australia

(Received 17 November 2002; published 10 June 2003)

Recent simulation work has established that the widely accepted mode-coupling theory for the strain rate dependence of the pressure and energy of simple fluids under shear (i.e., energy and pressure are functions of strain rate to the power  $\frac{3}{2}$ ) is observed in the vicinity of the triple point. Away from the triple point, the scaling exponent of the strain rate was seen to be closer to 2 than  $\frac{3}{2}$ , suggesting a possible analytic behavior. In this paper, we accurately determine the scaling exponent behavior for a Lennard-Jones fluid in the dense fluid region and find that it varies continuously between  $\sim 1.2$  and  $\sim 2$  as a function of density and temperature, thus confirming its nonanalyticity. We furthermore find that the behavior is characterized by a simple linear function of density and temperature.

DOI: 10.1103/PhysRevE.67.061201

PACS number(s): 61.20.Ja, 66.20.+d, 82.20.Wt, 83.50.Ax

In recent publications [1,2] we have demonstrated by non-equilibrium molecular dynamics (NEMD) simulations that the accepted behavior of simple fluids under planar shear flow, namely that the pressure and energy are linear functions of  $\dot{\gamma}^{3/2}$ , where  $\dot{\gamma}$  is the strain rate, is only strictly true in the vicinity of the triple point. In both these papers we showed that away from the triple point the behavior of the exponent in the strain rate was closer to 2, suggesting a possible analytic dependence. In this paper, we explore this scaling exponent dependence with greater precision and over a significant range of densities and temperatures, spanning the dense fluid region of the phase diagram for the Lennard-Jones fluid. We find a remarkably simple relationship clearly demonstrating that the scaling exponent is a continuous linear function of temperature and density. Significantly, the coefficients of these linear terms must be either universal or only dependent on the intermolecular potential. The exponent varies continuously between  $\sim 1.2$  and 2. There is thus nothing special about the  $\frac{3}{2}$  exponent predicted by the mode-coupling theory of Kawasaki and Gunton [3]. While it does occur near the triple point, it also occurs at higher density and temperature state points. That previous NEMD simulations have concurred with the mode-coupling prediction of a  $\frac{3}{2}$  exponent is a fortuitous consequence of performing simulations at the triple point. Agreement with the mode-coupling theory prediction breaks down at most other state points. This discovery indicates that there is a compelling need to reexamine the theoretical basis of the mode-coupling theory and either reformulate it such that it remains valid in the entire dense fluid phase, or else come up with an alternative theoretical foundation.

In our simulations, we have ensured to explore only the dense fluid phase. We note here that “fluid” in this strict sense may refer to liquid-vapor coexistence in some cases, but we have observed that this does not influence the shape of the strain rate profiles. We take care not to probe the liquid-solid coexistence region, as the strain rate profiles do not display simple power-law behavior in this region.

Our simulations are performed on a Lennard-Jones 6-12 fluid of 500 atoms. We use a cutoff of  $r_c = 3.5\sigma$ , which is a value often cited in the literature by other workers. To characterize the phase diagram for this cutoff, we perform Gibbs ensemble calculations for the liquid-vapor coexistence curve [4,5]. The solid-liquid coexistence is taken from the literature [6], and the phase diagram is presented in Fig. 1. Knowledge of the phase diagram ensures that we probe only the dense fluid region of the thermodynamic state space available to us in the weak field limit. The normal convention was adopted for the reduced density ( $\rho^* = \rho\sigma^3$ ), temperature ( $T^* = kT/\varepsilon$ ), energy ( $E^* = E/\varepsilon$ ), pressure ( $p^* = p\sigma^3/\varepsilon$ ), strain rate ( $\dot{\gamma}^* = [\sigma(m/\varepsilon)^{1/2}]\dot{\gamma}$ ), and time ( $\tau^* = [\varepsilon/m\sigma^2]^{1/2}\tau$ ). All quantities quoted in this work are in terms of these reduced quantities and the superscript asterisk will be omitted. Within the reduced temperature range of  $\sim 0.69$  to 1.25 we may safely conduct simulations between reduced densities of  $\sim 0.7$  to 0.84 and remain in the dense fluid region in the weak field limit.

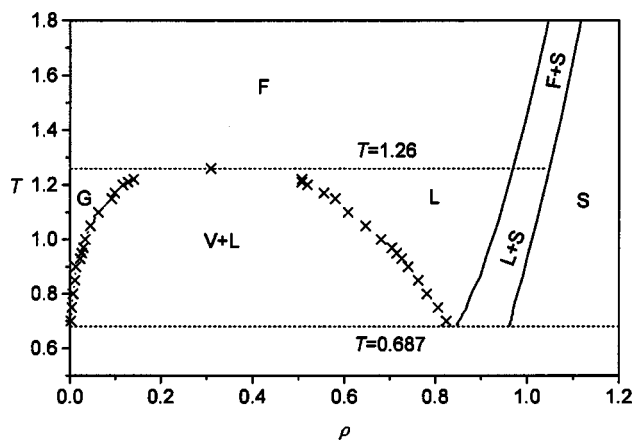


FIG. 1. Phase diagram for the 6-12 Lennard-Jones fluid with a cutoff radius of  $r_c = 3.5\sigma$ . The triple point is located at  $(\rho, T) = (0.85, 0.687)$ , in agreement with Ref. [6], and the critical point is estimated as  $(\rho, T) = (0.31, 1.26)$ . The solid-liquid line is also obtained from [6(b)]. The gas vapor, liquid, fluid, and solid phase regions are indicated by the symbols G, V, L, F, and S, respectively.

\*Author to whom correspondence should be addressed. E-mail address: btodd@swin.edu.au

Our NEMD simulations were conducted using the standard thermostatted Sllod<sup>1</sup> equations of motion [7], the details of which may be found in our previous work [1,2], and we use a Gaussian thermostat. Simulation run lengths varied according to the temperature/density requirements. For instance, simulations at low density (requiring long runs for good statistics) consisted typically of trajectories of 400 000 $\tau$ , where  $\tau=0.001$  is the time step. Averages of all quantities are then taken over 30–40 trajectories of this length. For high densities this could be reduced to  $\sim 10$  trajectories of 200 000 $\tau$  each while still preserving the same level of statistical accuracy. In all figures presented, error bars represent the standard error.

In what follows, we do not assume any value of the scaling exponent in either the energy or pressure (e.g.,  $\frac{3}{2}$  or 2), but determine its value *a priori* via a least-squares fit of the quantity (energy or pressure) as a function of strain rate. We assume only that the total energy and pressure observe a power-law dependence of the form

$$\begin{aligned} E &= E_0 + a \dot{\gamma}^\alpha, \\ p &= p_0 + b \dot{\gamma}^\alpha, \end{aligned} \quad (1)$$

where  $E_0$  and  $p_0$  are the total internal energy and pressure at equilibrium, and  $a$  and  $b$  are constants that depend on the density and temperature. This is certainly justifiable based on our previous work [1,2] and that of Matin *et al.* [8], and we typically find  $\chi^2 \sim 10^{-5}$  for the fits to the data presented in this paper. We then extract the value of  $\alpha$  for each  $(\rho, T)$  state point, where for each state point we probe the range  $0 \leq \dot{\gamma} \leq 0.6$  in steps of 0.1 reduced strain rate units (additional points were used to probe the Newtonian regime  $0 \leq \dot{\gamma} \leq 0.1$ ). This range encompasses both the Newtonian and non-Newtonian regimes. For simple fluids, a single exponent seems to be able to accurately describe the scaling behavior of the pressure and energy at any particular state point, within the range of uncertainties in our simulation data. Within these uncertainties we were unable to observe different power-law behavior for the Newtonian region within the strain rates  $0 \leq \dot{\gamma} \leq 0.1$ . This is clearly not the case for more complex polymeric fluids, in which different scaling exponents can be found in the Newtonian and non-Newtonian regimes (see, for example, Ref. [9]). Even if greater resolution were able to differentiate between different energy/pressure scaling parameters for the Newtonian and non-Newtonian regions in a simple fluid, our results are still valid in the non-Newtonian regime.

In Fig. 2 we plot the exponent  $\alpha$  computed for both the total potential energy per particle ( $U$ ) and pressure ( $p$ ) as a function of density for three different temperatures. Here  $U$  is defined as  $U = \sum_{i,j}^N u_{ij} / N$ , where  $u_{ij}$  is the interatomic potential energy between atoms  $i$  and  $j$ , and  $N$  is the total number of atoms in the simulation. The pressure is calculated as  $p = \frac{1}{3} \text{Tr}(\mathbf{P})$ , where  $\mathbf{P}$  is the pressure tensor [7]. We use po-

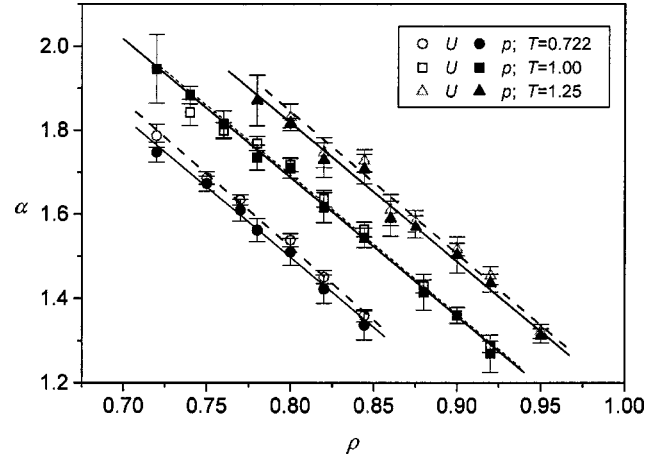


FIG. 2.  $\alpha$  as a function of density for different temperatures. All open symbols represent fits determined from the potential energy profile, whereas solid symbols refer to fits determined from the pressure profile.

tential energy to determine  $\alpha$  (rather than total energy) as the temperature is constrained to a constant value and thus does not contribute to the shape of the energy versus strain rate profile. The temperatures span the entire range of possible values wherein the fluid will remain in the dense fluid region over the range of densities studied. There are three significant features to note: (i) at all temperatures, the exponent  $\alpha$  is a *linear* function of density, maximum at low densities ( $\sim 2$ ), decreasing continuously to a minimum at high densities ( $\sim 1.2$ ); (ii) the value of  $\alpha$  is, within error bars, *identical* for both  $U$  and  $p$ ; and (iii) the dense liquid phase is clearly nonanalytic in strain rate. Furthermore, the widely accepted value of  $\alpha = \frac{3}{2}$  is only true in a *very small* region of the full available state space, lying in a range of densities between (0.8,0.9), depending on the temperature (increasing density with increasing temperature).

There is another significant feature to come out of this study. The exponent  $\alpha$  can be expressed as a simple linear function of *both* temperature and density:

$$\alpha = A + BT - C\rho, \quad (2)$$

where  $A$ ,  $B$ , and  $C$  are coefficients with the constant values  $A = 3.67 \pm 0.04$ ,  $B = 0.69 \pm 0.03$ , and  $C = 3.35 \pm 0.03$ . The values of  $A$ ,  $B$ , and  $C$  are either universally true for all single-component simple fluids (e.g.,  $\frac{11}{3}$ ,  $\frac{2}{3}$ , and  $\frac{10}{3}$ , respectively), or else must be functions only of the intermolecular potential. The significance of such a simple relationship is that it may now be possible to predict the pressure, stress, energy, etc., of at least simple nonequilibrium fluids as a function of strain rate at *any arbitrary* thermodynamic state point in the dense fluid phase. Equation (2) thus acts in an analogous way as an equation of state would, and can be used to characterize the scaling exponent  $\alpha$ .

We note here that we did not apply any long-range corrections to our pressure or energy calculations. This is in fact unnecessary, as the long-range correction would only shift the  $(p, U)$  values by a constant amount [10]; the shapes of the profiles (from which the  $\alpha$  are calculated) remain un-

<sup>1</sup>These equations are named Sllod because of the close relationship to the Dolls tensor algorithm.

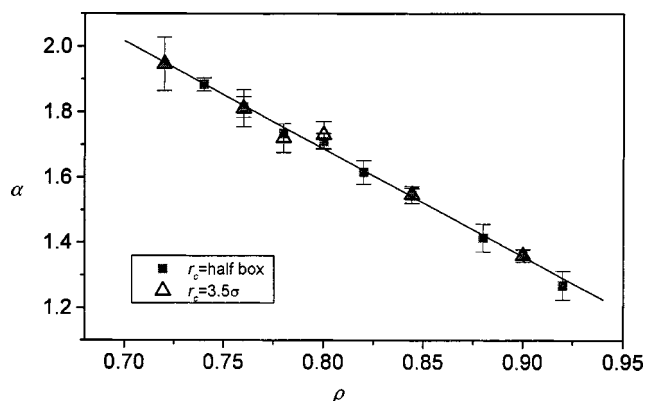


FIG. 3.  $\alpha$  as a function of density at  $T=1.0$  for cutoff values of  $r_c=3.5\sigma$  and  $r_c=L/2$ , where  $L$  is the simulation box length.

changed. However, to ensure that  $\alpha$  is independent of the value of cutoff used, we performed simulations at a cutoff of half the simulation box length,  $r_c=L/2$  at a fixed temperature of  $T=1.0$  over a range of liquid densities. Note that  $r_c$  will be different for each  $\rho$  studied. We compare the value of  $\alpha$  calculated for this system with those of our fixed cutoff ( $r_c=3.5\sigma$ ) in Fig. 3 and find perfect agreement.

A characteristic plot of  $\alpha$  computed for both  $U$  and  $p$  as a function of temperature at a fixed density of 0.8442 is shown in Fig. 4. As expected, the relationship is linear, but this time with a positive slope. Clearly, one could plot a three-dimensional curve in which  $\alpha$  is displayed as a function of  $T$  and  $\rho$ , but as the curve would in fact be a plane in thermodynamic state space there is no new insight to be gained by doing this.

Finally, to ensure that the fluid is indeed nonanalytic in strain rate, we also included the next allowable fourth-order term in the pressure and energy Taylor series expansions (proportional to  $\dot{\gamma}^4$ ) (see Ref. [2]), but found that the fit can be extremely poor at state points away from regions where  $\alpha\sim 2$ . We also tried fitting an exponential function to the data, with similarly poor results. We are thus confident that a simple power-law relationship is valid within the strain rates studied in this paper.

To conclude, we have fully characterized the shear rate scaling exponent behavior for the pressure and energy of simple atomic Lennard-Jones fluids. We find that the fluid is

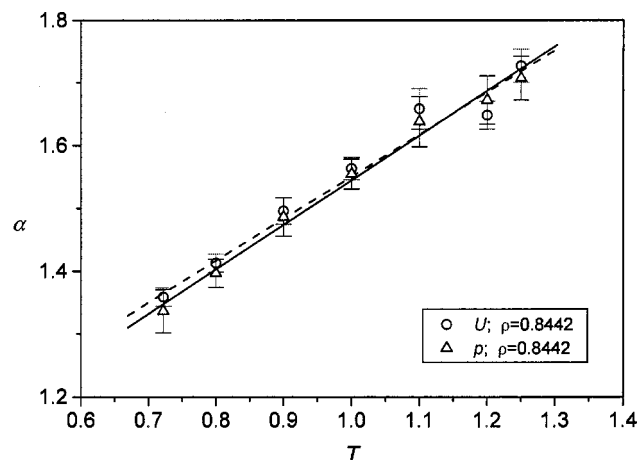


FIG. 4.  $\alpha$  as a function of temperature at  $\rho=0.8442$ . Circles represent fits obtained from the potential energy profile, and triangles represent fits obtained from the pressure profile.

nonanalytic in strain rate, but that the accepted  $\frac{3}{2}$  exponent has no special place in thermodynamic state space, occurring in a very limited region of relatively high density. A simple *single* linear relationship has been found that relates the exponent of *both* the pressure and energy strain rate profiles as a function of temperature and density. While it is likely that this linear relationship will be true for other intermolecular potentials (e.g., including those with three-body interaction terms), an intriguing question remains: are the values of the coefficients of Eq. (2) ( $A, B, C$ ) independent of intermolecular potential, and hence “universal,” or functions thereof? We are endeavoring to answer this question. It is hoped that our work will inspire other liquid state theorists to reexamine the mode-coupling theory of Kawasaki and Gunton and either attempt to extend its validity into wider regions of thermodynamic state space, or else invent an alternative theoretical framework to explain the observations reported here.

J.G. thanks the Australian government for financial support. G.W. thanks the School of Information Technology for financial support. We acknowledge the Swinburne Supercomputer Centre and the Australian Partnership for Advanced Computing for generous allocations of computer time.

- [1] G. Marcelli, B. D. Todd, and R. J. Sadus, *Phys. Rev. E* **63**, 021204 (2001).  
 [2] J. Ge, G. Marcelli, B. D. Todd, and R. J. Sadus, *Phys. Rev. E* **64**, 021201 (2001).  
 [3] K. Kawasaki and J. D. Gunton, *Phys. Rev. A* **8**, 2048 (1973).  
 [4] A. Z. Panagiotopoulos, *Mol. Phys.* **61**, 813 (1987).  
 [5] R. J. Sadus, *Molecular Simulation of Fluids: Theory, Algorithms and Object-Orientation* (Elsevier, Amsterdam, 1999).  
 [6] (a) D. A. Kofke, *J. Chem. Phys.* **98**, 4149 (1993); (b) R.

Agrawal and D. A. Kofke, *Mol. Phys.* **85**, 43 (1995).

- [7] D. J. Evans and G. P. Morriss, *Statistical Mechanics of Non-equilibrium Liquids* (Academic, London, 1990).  
 [8] M. Matin, P. J. Davis, and B. D. Todd, *J. Chem. Phys.* **113**, 9122 (2000).  
 [9] M. Kroger, W. Loose, and S. Hess, *J. Rheol.* **37**, 1057 (1993).  
 [10] M. P. Allen and D. J. Tildesley, *Computer Simulation of Liquids* (Oxford University Press, Oxford, 1987).